Inorganic Chemistry

ARTICLE

pubs.acs.org/IC

Porous Anionic, Cationic, and Neutral Metal-Carboxylate Frameworks Constructed from Flexible Tetrapodal Ligands: Syntheses, Structures, Ion-Exchanges, and Magnetic Properties

Tian-Fu Liu, Jian Lü, Chongbin Tian, Minna Cao, Zujin Lin, and Rong Cao*

State Key Laboratory of Structural Chemistry, Fujian Institute of Research on the Structure of Matter, Chinese Academy of Sciences, Fujian, Fuzhou, 350002, P. R. China

Supporting Information

ABSTRACT: A series of coordination polymers with anionic, cationic, and neutral metal-carboxylate frameworks have been synthesized by using a flexible tetrapodal ligand tetrakis[4-(carboxyphenyl)oxamethyl] methane acid (H_4X). The reactions between divalent transition-metal ions and H_4X ligands gave $[M_3X_2]\cdot[NH_2(CH_3)_2]_2\cdot 8DMA$ (M = Co (**1**), Mn (**2**), Cd(**3**)) which have anionic metal-carboxylate frameworks with $NH_2(CH_3)_2^+$ cations filled in channels. The reactions of trivalent metal ions Y(III), Dy(III), and In(III) with H_4X ligands afforded cationic metal-carboxylate frameworks $[M_3X_2\cdot(NO_3)\cdot(DMA)_2\cdot(H_2O)]\cdot 5DMA\cdot 2H_2O$ (M = Y(**4**), Dy(**5**)) and $[In_2X\cdot(OH)_2]\cdot 3DMA\cdot 6H_2O$ (**6**) with the NO_3^- and OH^- serving as counterions, respectively. Moreover, a neutral metal-carboxylate framework $[Pb_2X\cdot(DMA)_2]\cdot 2DMA$ (**7**) can also be isolated from reaction of Pb(II) and H_4X ligands. The charged metal-carboxylate frameworks **1**−**5** have selectivity for specific counterions in the reaction system, and compounds **1** and **2** display ion-exchange behavior. Moreover, magnetic property measurements on compounds **1**, **2**, and **5** indicate that there exists weak antiferromagnetic interactions between magnetic centers in the three compounds.

INTRODUCTION

Current interest in metal−organic frameworks (MOFs) not only stems from their potential applications in ferroelectrics, nonlinear optics, porous materials, and catalysis[1] but also from their intriguing varieties of molecular architectures and topologies.[2] The extensive research has led to numerous practical and conceptual developments in design and synthesis of MOFs, such as the "node and spacer" approach, secondary building unit (SBU), secondary building blocks (SBB), and reticular synthesis.[3] However, most of these methodologies are based on the initial requirement of conformational rigidity of the starting entities. It would be a difficult endeavor to try to synthesize predesigned MOFs from flexible ligands because the starting entities do not maintain their structural geometries during the self-assembly process. Meanwhile, in comparison with rigid ligands, the resultant structures are more sensitive to many subtle factors, and the syntheses and characterizations are somewhat more difficult. However, the flexibility of ligands is essential to form some particular properties and structures.[4] Furthermore, the flexibility of the ligands can afford a good opportunity to investigate the detail of a self-assembly process and provide more information for the directional synthesis of target MOFs. It is therefore an important aspect that is worthwhile paying attention to. Keeping this in mind, we selected flexible ligand tetrakis-[4-(carboxyphenyl)oxamethyl] methane acid (denoted as H_4X hereafter), in view of its flexible $-O-CH_2-$ moieties, to attempt to build porous MOFs and understand the factors which play profound roles on the formation of the thermodynamically favored products.

One of the features of metal carboxylate complexes is that the ligands are anionic, so the combination with metal centers can usually give neutral networks without counterions occupying the pores. However, the charged frameworks display some unique structures and properties prior to neutral ones.[5] For example, doping the metal ions (Li^+, Na^+, Mg^{2+}) into cavities, the electrostatic interaction sites can afford nondissociative H_2 binding to enhance overall adsorption of H_2.[6] Some of the charged frameworks exhibit selectivity or ion exchanges for specific ions,[7] and sometimes, structural transformations are involved in these processes. In our previous studies, the combination of H_4X ligands and Zn(II) ions gave three different neutral metal-carboxylate frameworks. Those compounds display second-harmonic generation (SHG), ferroelectric properties, hydrophilic affinity to the polar molecules, and $\pi-\pi$ interactions for aromatic molecules.[8] Some porous frameworks have also been obtained by other groups.[9] However, all the complexes are neutral metal-carboxylate frameworks. In the system of X ligand-based complexes, the incorporation of counterions in the charged metal-carboxylate frameworks has not been investigated. As a systematic research, we extend our work toward the investigation of charged metal-carboxylate frameworks derived from H_4X ligands with transition-metal ions, rare earth metal ions, and main group metal ions.

As usual, temperature, reaction duration, starting materials, pH, and auxiliary ligands are valid methods to control the structure and charge of the final frameworks. Herein the obtained complexes indicate that these compounds adapt their structural features, pore sizes, and framework charges to the metal ions and temperature without resorting to the change of solvent, pH, or auxiliary ligands. In this paper we report the solvothermal syntheses, structural characterizations, ion-exchanges, and magnetic

Received: September 20, 2010
Published: February 08, 2011

properties of seven MOFs based on H_4X ligands, namely, $[M_3X_2]\cdot[NH_2(CH_3)_2]_2\cdot 8DMA$ (M = Co (**1**), Mn (**2**), Cd(**3**)), $[M_3X_2\cdot(NO_3)\cdot(DMA)_2\cdot(H_2O)]\cdot 5DMA\cdot 2H_2O$ (M = Y (**4**), Dy (**5**)) $[In_2X\cdot(OH)_2]\cdot 3DMA\cdot 6H_2O$ (**6**), and $[Pb_2X\cdot(DMA)_2]\cdot$ 2DMA (**7**).

EXPERIMENTAL SECTION

General. All chemicals were commercially purchased and used without further purification. Elemental analyses (C, N, and H) were carried out with an Elementar Vario EL III analyzer; Na and K in the exchanged samples were determined by a Jobin Yvon Ultima2 inductively coupled plasma OES spectrometer. IR spectra were recorded with PerkinElmer Spectrum One as KBr pellets in the range 400−4000 cm^{-1}. Single crystal X-ray diffraction was carried out by a Rigaku Mercury CCD/AFC diffractometer. Thermogravimetric analysis (TGA) was carried out on a NETZSCH STA 449C instrument. The sample and reference (Al_2O_3) were enclosed in a platinum crucible and heated at a rate of 10 °C/min from room temperature to 1000 °C under nitrogen atmosphere.

Synthesis of $[Co_3X_2]\cdot[NH_2(CH_3)_2]_2\cdot 8DMA$ (**1**). A mixture of $Co(NO_3)_2\cdot 6H_2O$ (0.058 g 0.2 mmol), H_4X (0.06 g, 0.1 mmol), and 10 mL DMA was sealed in an autoclave equipped with a Teflon linear (23 mL), heated at 90 °C for 4 days, and then cooled to room temperature. Purple block single crystals of **1** were collected in a ca. 82% yield based on H_4X. Elemental analysis for $C_{102}H_{136}N_{10}Co_3O_{32}$, calcd (%): C, 55.87; H, 6.21; N, 6.39. Found (%). C, 56.34; H, 6.35; N, 6.27. IR data (KBr, cm^{-1}): 3444 (w), 1606 (s), 1397 (s), 1239 (s), 1019 (m), 785 (m).

Synthesis of $[Mn_3X_2]\cdot[NH_2(CH_3)_2]_2\cdot 8DMA$ (**2**). The complex was prepared by similar procedure used for preparation of **1** except that $Mn(NO_3)_2\cdot 6H_2O$ (0.057 g 0.2 mmol) was used instead of $Co(NO_3)_2\cdot 6H_2O$. Colorless block single crystals of **2** were collected in a ca. 86% yield based on H_4X. Elemental analysis for $C_{102}H_{136}N_{10}Mn_3O_{32}$, calcd (%): C, 56.17; H, 6.24; N, 6.42. Found (%): C, 55.65; H, 6.07; N, 6.73. IR data (KBr, cm^{-1}): 3413 (w), 1606 (s), 1396 (s), 1241 (s), 1015 (m), 786 (m).

Synthesis of $[Cd_3X_2]\cdot[NH_2(CH_3)_2]_2\cdot 8DMA$ (**3**). The complex was prepared by similar procedure used for preparation of **1** except that $Cd(NO_3)_2\cdot 4H_2O$ (0.062 g, 0.2 mmol) was used instead of $Co(NO_3)_2\cdot 6H_2O$. Colorless block single crystals of **3** were collected in a ca. 88% yield based on H_4X. Elemental analysis for $C_{102}H_{136}N_{10}Cd_3O_{32}$, calcd (%): C, 52.06; H, 5.78; N, 5.96. Found (%): C, 51.09; H, 5.39; N, 5.22. IR data (KBr, cm^{-1}): 3444 (w), 1606 (s), 1395 (s), 1243 (s), 1015 (m), 784 (m).

Synthesis of $[Y_3X_2\cdot(NO_3)\cdot(DMA)_2\cdot(H_2O)]\cdot 5DMA\cdot 2H_2O$ (**4**). A mixture of $Y(NO_3)_3\cdot 5H_2O$ (0.087 g, 0.2 mmol), H_4X (0.06 g, 0.1 mmol) and 10 mL DMA was sealed in an autoclave equipped with a Teflon linear (23 mL), heated at 110 °C for 4 days, and then cooled to room temperature. Colorless block single crystals of **4** were collected in a ca. 76% yield based on H_4X. Elemental analysis for $C_{94}H_{117}N_8O_{37}Y_3$, calcd (%): C, 51.88; H, 5.28; N, 5.05. Found (%): C, 52.18; H, 5.41; N, 4.88. IR data (KBr, cm^{-1}): 3359 (w), 1606 (s), 1420 (s), 1243 (s), 1014 (m), 785 (m).

Synthesis of $[Dy_3X_2\cdot(NO_3)\cdot(DMA)_2\cdot(H_2O)]\cdot 5DMA\cdot 2H_2O$ (**5**). The complex was prepared by similar procedure used for preparation of **4** except that $Dy(NO_3)_3\cdot 5H_2O$ (0.076 g 0.2 mmol) was used instead of $Y(NO_3)_3\cdot 5H_2O$. Colorless block single crystals of **5** were collected in a ca. 88% yield based on H_4X. Elemental analysis for $C_{94}H_{117}N_8O_{37}Dy_3$, calcd (%): C, 46.27; H, 4.80; N, 4.59. Found (%): C, 45.12; H, 5.12; N, 4.79. IR data (KBr, cm^{-1}): 3406 (w), 1606 (s), 1415 (s), 1245 (s), 1021 (m), 784 (m).

Synthesis of $[In_2X\cdot(OH)_2]\cdot 3DMA\cdot 6H_2O$ (**6**). The complex was prepared by similar procedure used for preparation of **1** except that $In(NO_3)_3\cdot 4H_2O$ (0.076 g, 0.2 mmol) was used instead of $Co(NO_3)_2\cdot 6H_2O$. Colorless block single crystals of **6** were collected in a ca. 69% yield based on H_4X. Elemental analysis for $C_{45}H_{65}N_3In_2O_{23}$, calcd (%): C, 42.78; H, 5.02; O, 29.12; N, 3.45. Found (%): C, 43.37; H, 5.22; O, 29.56; N, 3.37. IR data (KBr, cm^{-1}): 3446 (w), 1607 (s), 1412 (s), 1244 (s), 1015 (m), 784 (m).

Synthesis of $[Pb_2X\cdot(DMA)_2]\cdot 2DMA$ (**7**). The complex was prepared by similar procedure used for preparation of **4** except that $Pb(NO_3)_2$ (0.066 g 0.2 mmol,) was used instead of $Y(NO_3)_3\cdot 5H_2O$. Colorless block single crystals of **7** were collected in a ca. 72% yield based on H_4X. Elemental analysis for $C_{49}H_{42}N_4O_{16}Pb_2$, calcd (%): C, 43.33; H, 3.10; N, 4.13. Found (%): C, 42.98; H, 3.25; N, 4.43. IR data (KBr, cm^{-1}): 3390 (w), 1606 (s), 1403 (s), 1240 (s), 1173 (m), 785 (m).

Single Crystal Structure Determination. Data for complexes **1**−**7** were collected on a Rigaku Mercury CCD/AFC diffractometer equipped with graphite-monochromated Mo Kα radiation with a radiation wavelength of 0.71073 Å by using the ω-scan technique. All absorption corrections were performed using the CrystalClear program.[10] Structures were solved by direct methods and refined on F^2 by full matrix least-squares using the SHELXL-97 program package.[11] The organic hydrogen atoms were positioned geometrically. The hydrogen atoms bonded to solvent atoms were not located. Restraints for the bond distances were used during the refinement for keeping the suitable bond distances of disordered solvent molecules. Because of the highly disordered solvent molecules in compounds **1**, **3**, and **6**, the SQUEEZE routine in the PLATON software was applied to subtract the diffraction contribution from the solvent molecules.[12] Compounds **1**−**3** are isostructural, so they have identical formulas. According to elemental analytic data, IR spectrum, and TGA analysis, the solvent molecules of compound **6** were proposed to be approximately 3DMA and $6H_2O$ per formula. Details of the structure solution and final refinements for the complexes are given in Table 1. Selected bonds are in Table S1(Supporting Information). CCDC 793864−793869 and 804657 contain the crystallographic data (**1**−**4**, **6**, **7**, and **5**, respectively) for this paper. These data can be obtained from the Cambridge Crystallographic Date Center via www.ccdc.cam.ac.uk.

RESULTS AND DISCUSSION

Crystal Structure of $[M_3X_2]\cdot[NH_2(CH_3)_2]_2\cdot 8DMA$ (M = Co (1), Mn (2), Cd (3)). Complexes **1**−**3** are isostructural. As a representative example, the crystal structure of compound **2** is depicted here in detail. The asymmetric unit consists of two crystallographically independent Mn(II) ions, a X^{4-} ligand, four DMA solvent molecules, and an $NH_2(CH_3)_2^+$ counterion. The $NH_2(CH_3)_2^+$ is generated via either hydrolysis or decarbonylation of DMA under a solvothermal condition and is not without precedent.[13] Mn(1) ion is bonded by four oxygen atoms from two chelating carboxyl groups and two oxygen atoms from two bridging carboxyl groups giving an octahedral geometry. Mn(2) is also six coordinated by four oxygen atoms from four bridging carboxyl groups and two μ_3-O atoms from chelating bridging carboxyl groups to give a very distorted octahedron. Meanwhile, Mn(2) lies on an inversion center and connects to two neighboring Mn(1) centers by a pair of μ_3-O atoms in a vertex-sharing mode forming a trimetallic cluster. The X^{4-} ligands adopt distorted tetrahedral geometries with the angles between four arms ranging from 58° to 140°. Fourteen arms from five ligands and four metallic clusters compose a box-like mesopore which is filled by solvent molecules and counterions (Figure 1b). These mesoporous structures propagate to a porous three-dimensional (3D) framework with two kinds of channels, A (10.1 × 10.5 $Å^2$) and B (13.1 × 16.3 $Å^2$) along the [100] direction (Figure 1c). Complex **2** has a total solvent-accessible volume of 49.8%, as calculated using the PLATON routine.

dx.doi.org/10.1021/ic1019229 |*Inorg. Chem.* 2011, 50, 2264–2271

Table 1. Crystal Data and Data Collection and Refinement Parameters for Complexes

complexes	1	2	3	4	5	6	7
formula	$C_{102}H_{136}N_{10}Co_3O_{32}$	$C_{102}H_{136}N_{10}Mn_3O_{32}$	$C_{102}H_{136}N_{10}Cd_3O_{32}$	$C_{94}H_{117}N_8Y_3O_{37}$	$C_{94}H_{117}N_8Dy_3O_{37}$	$C_{45}H_{63}N_3In_2O_{23}$	$C_{49}H_{42}N_4Pb_2O_{16}$
formula weight	2191	2179	2351	2217	2438.49	1245	1375
temperature (K)	293(2)	293(2)	293(2)	293(2)	78(2)	293(2)	293(2)
wavelength (Å)	0.71073	0.71073	0.71073	0.71073	0.71073	0.71073	0.71073
crystal system	triclinic	triclinic	triclinic	orthorhombic	orthorhombic	monoclinic	orthorhombic
space group	P-1	P-1	P-1	*Pbcm*	*Pbcm*	*C2/c*	*Pbcn*
a (Å)	11.868(7)	11.775(3)	11.970(3)	10.6762(2)	10.7029(2)	19.651(5)	7.008(2)
b (Å)	16.265(1)	16.113(5)	16.341(5)	28.242(5)	28.176(5)	38.598(8)	30.224(9)
c (Å)	16.379(1)	16.346(5)	16.436(5)	34.079(6)	34.014(6)	21.519(5)	24.257(7)
α (°)	108.099(7)	108.244(2)	107.913(2)	90	90	90	90
β (°)	102.855(6)	101.663(4)	103.400(4)	90	90	117.068(4)	90
γ (°)	101.216(3)	102.559(2)	100.533(2)	90	90	90	90
volume ($Å^3$)	2808.7(1)	2750.1(1)	2861.4(1)	10276(3)	10257(3)	14534(6)	5138(3)
Z	1	1	1	4	4	8	4
Dc (Mg/m^3)	0.874	1.262	0.951	1.357	1.527	0.799	1.778
μ (mm^{-1})	0.487	0.418	0.601	1.765	2.247	0.667	6.617
data collected	24190	21398	22497	77435	61188	62821	37339
unique data (R_{int})	12617	11767	13068	11898	9643	16521	5890
parameters	450	715	487	696	786	434	245
goodness-of -fit on F^2	0.937	1.048	1.002	1.004	1.011	1.034	1.132
R_1[a] $[I > 2\sigma(I)]$	0.0836	0.0707	0.0460	0.0852	0.0768	0.0635	0.0500
wR_2[b]	0.2376	0.1853	0.1442	0.2349	0.1592	0.1810	0.1116

[a] $R_1 = \sum||F_0| - |F_c||/\sum|F_0|$. [b] $wR_2 = \{\sum[w(F_0^2 - F_c^2)^2]/\sum[w(F_0^2)^2]\}^{1/2}$.

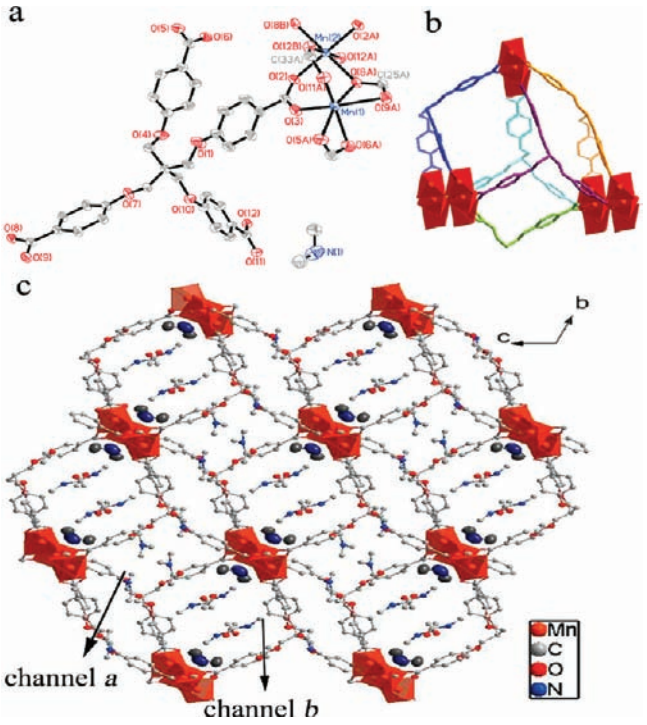

Figure 1. (a) ORTEP drawing of ligand and coordination environments of metal ions with thermal ellipsoids at 30% probability in compound **1**. (b) The box-like mesopore composed by trimetallic clusters and ligands. (c) The porous framework with channels A and B.

Crystal structure of $[M_3X_2\cdot(NO_3)\cdot2(DMA)\cdot(H_2O)]\cdot5DMA\,2H_2O$ (M = Y (4), Dy (5)). Complexes **4** and **5** are isostructural, and the crystal structure of compound **4** is depicted here in detail. The asymmetric unit of **4** consists of half-occupied Y(1) and Y(2) atoms on the mirror plane, one full-occupied Y(3) in a general position, one X^{4-} ligand, two full DMA molecules, and three halves of DMA molecules as well as half of a NO_3^- as a counterion. Y(1) and Y(2) centers are seven coordinated by six oxygen atoms from six bridging carboxyl groups and one oxygen atom from a DMA molecule, to give monocapped triprismatic geometries. Y(3) center, which displays monocapped triantiprismatic geometry, bonds to four oxygen atoms from four carboxyl groups, two oxygen atoms from a nitrate group, and one water molecule. All the carboxyl groups link adjacent Y(III) centers in a bridging bis-bidentate mode forming a 1D Y-carboxyl chain, and the NO_3^- counterions hang on both sides of the chain (Figure 2). The chains run parallel to the *b* axis and are connected into a 3D porous framework by X^{4-} ligands. The X^{4-} ligands adopt severely distorted tetrahedral orientations with the angles between the four arms ranging from 66° to 144°. Topological simplification using TOPOS software[14] indicates that it is a 4, 6, 8-connected net with point (Schläfli) symbol $(4^{13}.6^2)_2(4^{19}.6^9)_2(4^4.6^2)$, upon considering X^{4-} ligands as eight-connected nodes, and Y(III) atoms as four- and six-connected nodes (Figure 3). The pore system has a solvent accessible void of 46.3% (on removal of coordinated and uncoordinated DMA molecules).

Crystal structure of $[In_2X\cdot2(OH)]\cdot3DMA\cdot6H_2O$ (6). The asymmetric unit of **6** consists of an X^{4-} ligand, three In(III) ions and two OH^- as counterions. The half-occupied In(1) and In(3) atoms sit on the inversion centers, and the full-occupied In(2) atom sits on a general position. All the In(III) centers are six coordinated by four oxygen atoms from four bridging carboxyl groups and two OH^- forming octahedral coordination spheres

dx.doi.org/10.1021/ic1019229 |*Inorg. Chem.* 2011, 50, 2264–2271

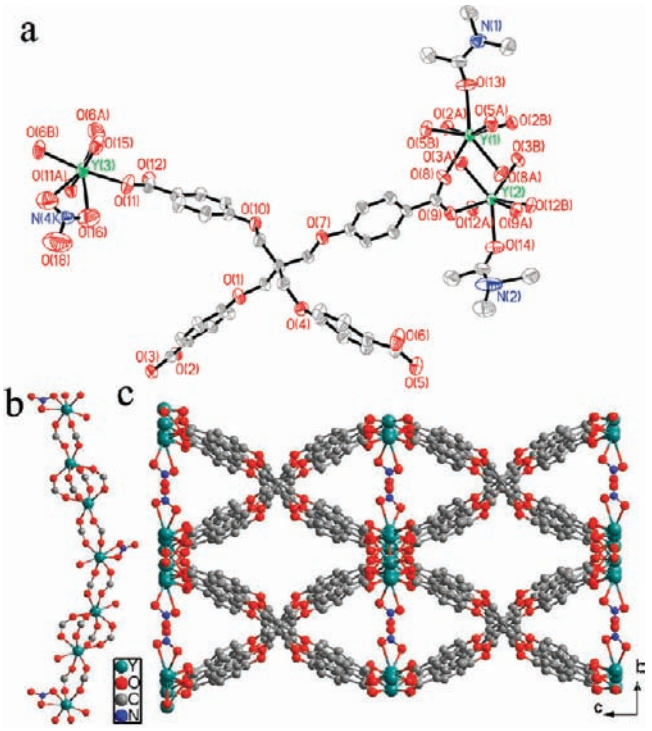

Figure 2. (a) ORTEP drawing of ligand and coordination environments of metal ions with thermal ellipsoids at 30% probability in **4**. (b) The metal-carboxyl chain in **4** and (c) the 3D porous structure presents in **4**.

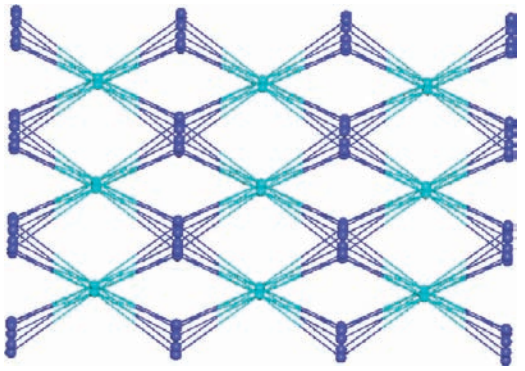

Figure 3. Topological presentation of **4** (the X^{4-} is indicated in aqua, and Y(III) is indicated in blue).

with the In−O distances ranging from 2.091 to 2.160 Å. Adjacent $\{InO_6\}$ octahedra are interconnected in the vertex-sharing mode forming an undulating In−O chain (Figure 4). The tetrahedral X^{4-} connectors, with the angles between the four arms ranging from 76° to 133°, link together three neighboring In−O chains to give a porous framework with channels along both [100] and [001] directions. The largest channels are 19.6 × 10.1 $Å^2$ in cross-section and present in [001] direction, as shown in Figure 4. In the X-ray structure refinement, however, guest molecules could not be located because of their high thermal disorder, and the final structure model was refined without the solvent molecules by using a SQUEEZE routine of PLATON. Meanwhile, the solvent accessible void space estimated by PLATON is 67%, which is filled with three DMA and six H_2O guest molecules per unit formula of the host as evidenced by the element analysis and TGA data.

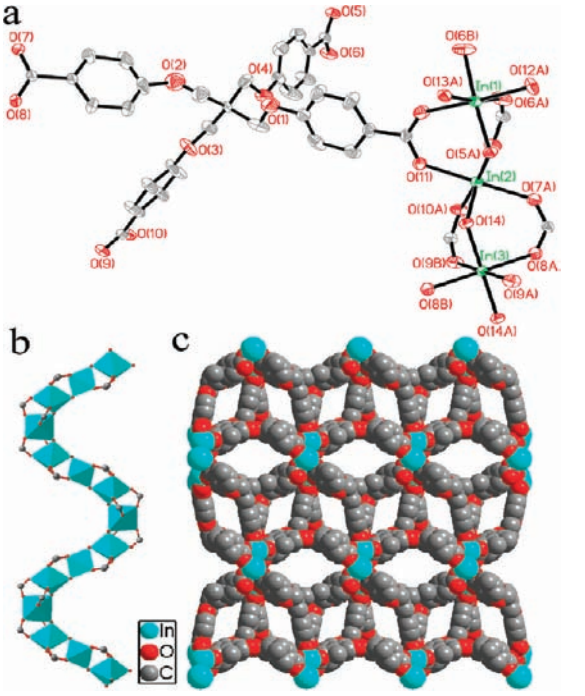

Figure 4. (a) ORTEP drawing of ligand and coordination environments of metal ions with thermal ellipsoids at 30% probability in compound **6**. (b) Polyhedral view of the undulating In−O chain. (c) Space-filling view of **6** showing large channels.

Crystal structure of $[Pb_2X\cdot(DMA)_2]\cdot 2DMA$ (7). The asymmetric unit of **7** consists of one Pb(II) atom, a half of a X^{4-} ligand, and two DMA molecules. The central Pb(II) ion adopts a distorted $\{:PbO_6\}$ pentagonal−bipyramidal geometry by coordinating to four oxygen atoms from two chelating carboxyl groups, a μ_3-O atom from a chelating bridging carboxyl group and an oxygen atom from a DMA molecule, and the seventh coordination site is occupied by the lone pair of electrons. The Pb−O distances are in the range of 2.359−2.781 Å, which is within the range observed in other Pb(II) complexes.[15] As a heavy *p*-block metal ion, the lead has a large atomic radius and a flexible coordination environment which provides unique opportunities for the formation of versatile network topologies. In compound **7**, each Pb(II) center is connected to adjacent metal ions by a pair of μ_3-O atoms giving an infinite 1D Pb−O chain. Such four neighboring chains are connected by the tetrapodal X^{4-} ligands into a clathrate neutral porous framework, and the DMA molecules (solvent and coordinated) filled in the voids (Figure 5). The ligands adopt a nearly flattened orientation with angles between four arms ranging from 84° to 151°. The solvent accessible volume is 2465 $Å^3$ per unit cell, which is 48.0% of the total crystal volume (calculated by PLATON on removal of coordinated and uncoordinated DMA molecules). Topological simplification using TOPOS software indicates that the compound is a 3, 6-connected net with point (Schläfli) symbol $(4.8^2)_2$-$(4^2.8^{12}.10)$. Each X^{4-} ligand connects to six Pb(II) atoms affording a six-connected node, and each Pb(II) ion links to three X^{4-} ligands affording a three-connected node, as shown in Figure 6.

DISCUSSION

Complexes **1**−**7** were obtained by reaction of X^{4-} ligands with transition-metal ions, rare earth metal ions, and main group

dx.doi.org/10.1021/ic1019229 |*Inorg. Chem.* 2011, 50, 2264–2271

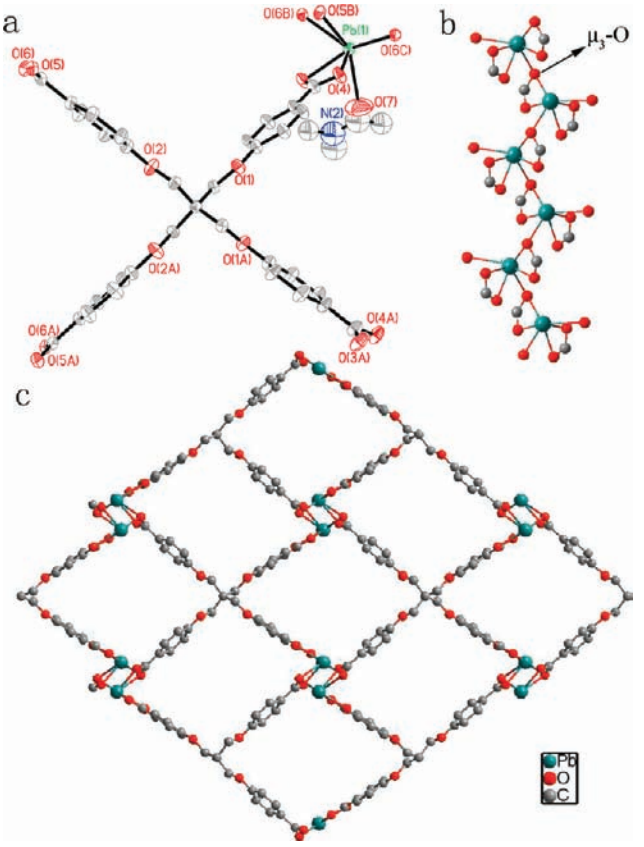

Figure 5. (a) ORTEP drawing of ligand and coordination environment of metal ion with thermal ellipsoids at 30% probability in compound **7**. (b) The Pb−O chain linked by μ_3-O. (c) The 3D porous structure present in **7**.

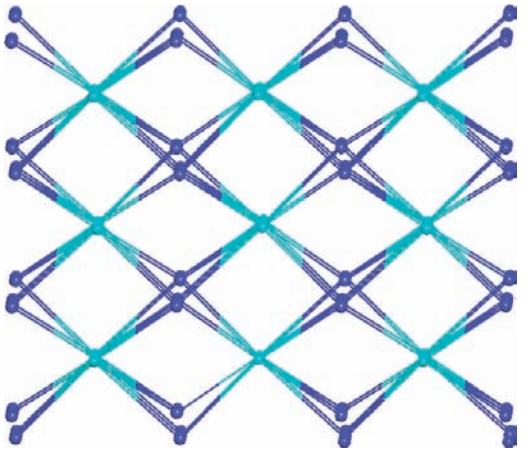

Figure 6. Topological presentation of **7** (the X^{4-} is indicated in aqua and Pb(II) is indicated in blue).

metal ions. The metal centers of the resultant compounds varied from trimetallic cluster (**1**−**3**) and metal-carboxyl chain (**4** and **5**) to metal-O chain (**6** and **7**). The tetrapodal X^{4-} ligands adopt different geometries varying from tetrahedral to nearly flattened. Those factors that lead to the networks have differences in solid-state packing, topology, and porosity, and the obtained metal-carboxylate frameworks can be anionic, cationic, and neutral, which have selectivity toward

Scheme 1. Schematic Representation of the Self-Assembly of X^{4-} Ligands and Different Metal Ions with Selectivity for Counterions

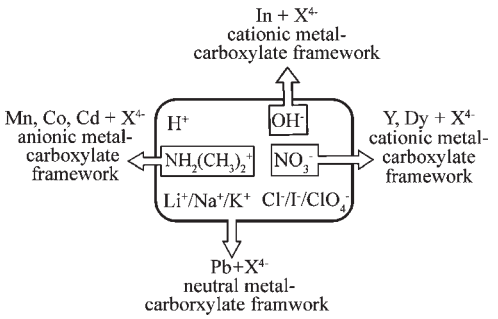

counterions in the reaction system. For compounds **1**−**3**, the divalent metal centers are six coordinated in octahedral geometries. All the coordinated oxygen atoms come from the carboxyl groups. Completing the coordination geometries of metal centers, the carboxyl groups introduce surplus negative charges. In this case, the uncoordinated, $NH_2(CH_3)_2^+$ cations are found to act as counterions. For trivalent metal complexes **4**−**6**, Y(III) (Dy(III)) are seven coordinated, and the In(III) is six coordinated. The carboxyl groups can neither complete the coordination geometry nor satisfy the charge balance. As a result, NO_3^- and OH^- ions, which cannot only coordinate to metal center but also provide negative charge, are observed to be incorporated in the frameworks. It can be proposed that the metal ions with higher charge and coordination numbers will be more liable to construct cationic metal-carboxylate frameworks.

In order to further understand the selectivity for specific ions, we have sought to generate the analogues of complexes **1**−**5** with various counterions. When the $LiNO_3$ (or $NaNO_3$, KNO_3) was added as starting material in the reaction system for **1**−**3**, the single-crystal X-ray diffraction, energy-dispersive system (EDS), and powder X-ray diffraction (PXRD) indicated that **1**−**3** were recovered without Li^+ (or Na^+, K^+) substituting $NH_2(CH_3)_2^+$ ions. Similarly, in the reaction system for **4** and **5**, the addition of KCl (or KI, $KClO_4$) did not lead to a change of the product. The Cl^- (or I^-, ClO_4^-) could not be combined as counterions instead of NO_3^-, as testified by EDS and PXRD. Although they are the same in charge, different geometries and affinities to metal centers cause them not to be substituted in the process of self-assembly (Scheme 1).

Ion-Exchange. Freshly prepared crystals of **1** were introduced into a saturated aqueous solution of $NaNO_3$ (5 mL). Five mL DMA containing pH-sensitive compound, phenolphthalein (30 mg), was added. The solution was adjusted to pH = 8 by adding tetramethylammonium hydroxide solution following with the color change from colorless to pink. The sample was heated at 45 °C for 48 h, after that, the color faded out, and the pH value decreased to 7 indicating the increase of the protons in the solution. Exchanged sample **1a** was filtered and washed with water and ethanol several times. The crystals turned opaque and diffracted too weakly to give structural information. However, inductively coupled energy (ICP) analysis of **1a** reveals that it contains Na^+ 2.18%, which means that the $NH_2(CH_3)_2^+$ cations within the channels of **1** can be replaced by the Na^+ ions in the solution driven by the concentration gradient. Figure 7 represents the process and ICP results of the ion-exchange experiments for

dx.doi.org/10.1021/ic1019229 |*Inorg. Chem.* 2011, 50, 2264–2271

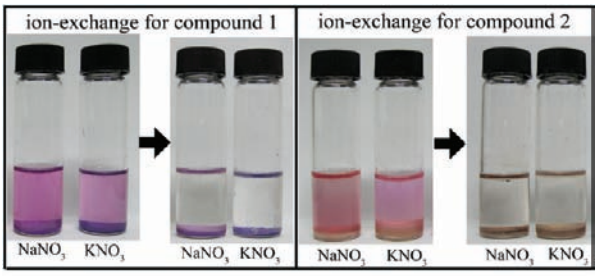

	Compound 1	Compound 2
Na^+	2.18%	3.17%
K^+	3.43%	3.58%

Figure 7. Photos of the ion-exchange process (top). The list of ICP results for the ion exchanged samples of **1** and **2** (bottom).

compounds **1** and **2** in $NaNO_3$ and KNO_3 solutions, respectively. The Figure S1 (in Supporting Information) is the IR spectra of compounds **1** and **2** before and after ion-exchange. This experiment establishes that ion-exchange can be successful in a porous framework. Although the replacement of $NH_2(CH_3)_2^+$ by other ions is unfeasible in the self-assembly process, it can be finished by the ion-exchange experiment conducted on the obtained compound. This work may exploit a facile entry for an incorporation specified component into a complex for the preconceived need in material design.

Magnetic Properties. Variable-temperature magnetic measurements were performed on polycrystalline samples of compounds **1**, **2**, and **5** at an applied magnetic field of 1000 Oe over the temperature range from 2 to 300 K. The temperature dependence of the magnetic susceptibility of **1** is shown in Figure 8a. The $\chi_m T$ value at room temperature is 9.04 $cm^3\ mol^{-1}$ K and substantially exceeds that of the spin-only value of 5.63 $cm^3\ mol^{-1}$ K expected for three isolated octahedral coordinated Co(II) ions.[16] Upon cooling, the $\chi_m T$ value first decreases gradually to a minimum of 7.01 $cm^3\ mol^{-1}$ K at 12.4 K (indicating a dominant antiferromagnetic interaction and/or spin-obit coupling of the Co(II) ions) and then increases sharply to 9.86 $cm^3\ mol^{-1}$ K at about 2 K. The reciprocal susceptibility versus temperature plot above 15 K obeys the Curie−Weiss law with $C = 9.05\ cm^3\ mol^{-1}$ K and $\theta = -8.76$ K. To quantitatively evaluate the isotropic magnetic interaction between spin carriers, the data above 50 K were fitted to the expression of susceptibility for linear trinuclear Co(II) systems deduced from the Hamiltonian $H = -J_{12}S_1 \times S_2 - J_{23}S_2 \times S_3 - J_{13}S_1 \times S_3$. Based on the structural information of the perfect symmetry of the trimer and the long distance (7.214 Å) between the terminal metal centers, we can take the coupling J_{12} and J_{23} to be identical and the coupling between the terminal metal centers J_{13} to be zero. So the exchange Hamiltonian can be expressed as $H = -J(S_1 \times S_2 - S_2 \times S_3)$.[17] The best fit of the data was obtained with the parameters $J = -2.11 \pm 0.02\ cm^{-1}$, $g = 2.59 \pm 0.001$ and R, defined as $R = \sum[(\chi_m T)_{obs} - (\chi_m T)_{calc}]^2 / \sum[(\chi_m T)_{obs}]^2$, equal to 1.34×10^{-3}. An attempt to take into account the intertrimetallic cluster coupling zJ' which would improve the fitting was not realized. This indicates that the interactions between the trimetallic clusters are very weak due to the very long distance of the trimetallic clusters.

The $\chi_m T$ value of compound **2** at room temperature is 12.8 $cm^3\ mol^{-1}$ K which corresponds to the spin-only value expected for three isolated Mn(II) ions (13.125 $cm^3\ mol^{-1}$ K, $3d^5$, $S = 5/2$, $g = 2$). The $\chi_m T$ value decreases to 4.23 $cm^3\ mol^{-1}$ K as the temperature cools down (Figure 8b). Fitting the magnetic data

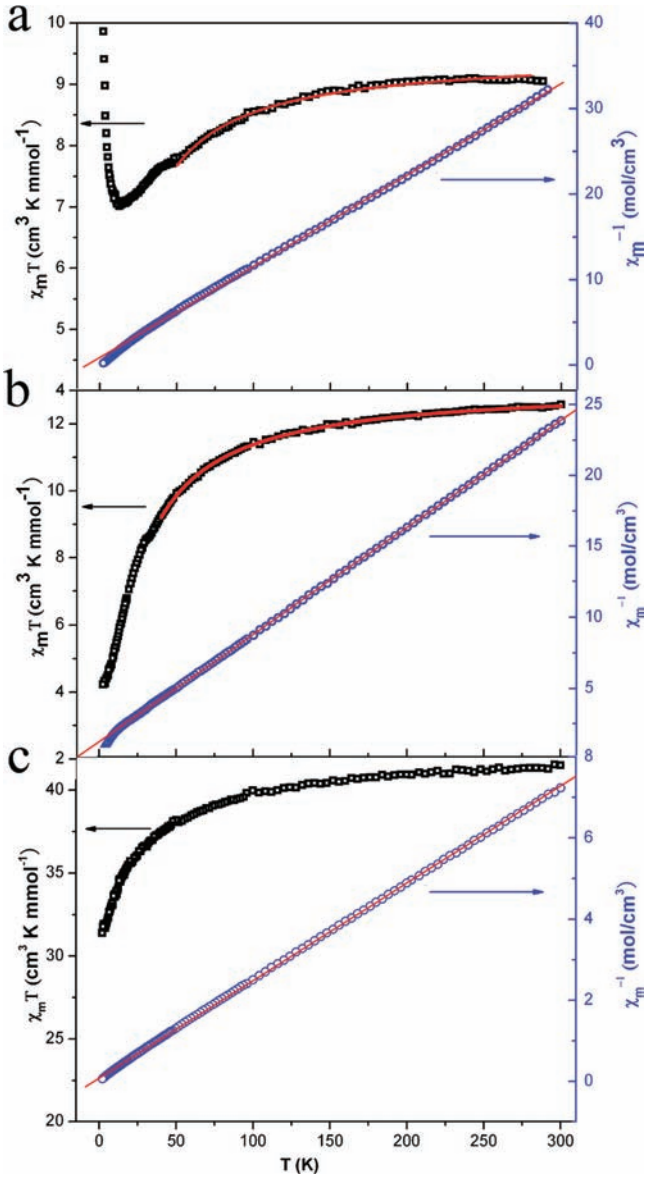

Figure 8. Plot of the $\chi_m T$ and χ_m^{-1} versus T for **1** (a), **2** (b), and **5** (c). The red solid lines represent the best fit obtained from the Hamiltonian given in the text and Curie−Weiss law.

according to the Curie−Weiss law in the range of 10−300 K gave a negative Weiss constant of −16.75 K, indicating weakly antiferromagnetic behavior. The Mn1 and Mn2 and the Mn2 and Mn1′ distance is 3.497 Å, Mn1 and Mn1′ distance is 6.993 Å, so the exchange Hamiltonian can also be expressed as $H = -J(S_1 \times S_2 - S_2 \times S_3)$.[18] The $\chi_m T$ vs T plot fit reasonably well in the temperature range of 40−300 K with the parameters $J = -1.25 \pm 0.004\ cm^{-1}$ and $g = 2.00 \pm 0.0005$ and with an agreement factor $R = 6.6 \times 10^{-4}$. The negative J values are comparable to the previous reported compounds with the similar structure.[18] Moreover, compounds **1** and **2** retain their magnetic properties after ion-exchange experiments (Figure S2 in Supporting Information).

The plot of $\chi_m T$ versus T for compound **5** is shown in Figure 8c. The room temperature $\chi_m T$ values were measured as 41.48 $cm^3\ mol^{-1}$ K, which is in good agreement with the expected value for three isolated Dy(III) ions (42.53 $cm^3\ mol^{-1}$ K,

dx.doi.org/10.1021/ic1019229 |Inorg. Chem. 2011, 50, 2264–2271

$^6H_{15/2}$, $S = 5/2$, $L = 5$, $g = 4/3$). It shows a continuously steady decrease upon lowering the temperature, falling to 31.38 cm^3 mol^{-1} K at 2 K. The magnetic data obey the Curie−Weiss law with $C = 41.68$ cm^3 mol^{-1} K and a negative Weiss constant of −3.67 K. Such magnetic behaviors of decrease $\chi_m T$ and negative value of θ, typical for Ln(III) complexes, are primarily due to splitting of the ligand field for the Ln(III) ions as a result of strong spin−orbital coupling and partly attributed to the possible antiferromegnetic intradimer coupling.[19]

CONCLUSIONS

In conclusion, we have successfully synthesized seven porous metal carboxylate complexes from flexible tetrapodal ligands and transition-metal ions, rare earth metal ions, and main group metal ions. This study has shed some light on the roles different metal ions play in the formation of self-assembly frameworks. The coordination of divalent transition-metal ions with X^{4-} ligands produces anionic metal-carboxylate frameworks **1**−**3** with $NH_2(CH_3)_2^+$ counterions filled in void spaces. Whereas, the coordination of trivalent rare earth metal ions Y(III) and Dy(III) and main group metal ion In(III) with X^{4-} ligands produces cationic metal-carboxylate frameworks **4**−**6** with NO_3^- and OH^- combined as counterions, respectively. It can be proposed that the metal ions with higher charge and coordination numbers will be more liable to construct cationic metal-carboxylate frameworks. Meanwhile, the neutral metal-carboxylate framework **7** can also been obtained by employing Pb(II) and X^{4-} ligands. The addition of other ions did not lead to a change of products (**1**−**5**), and the counterions could not be replaced by other ions although they are the same in charge. The observation indicates those complexes have selectivity for specific counterions in the self-assembly process. More interestingly, the $NH_2(CH_3)_2^+$ in the channels of compounds **1** and **2** displays ion-exchange behaviors when treated with saturated $NaNO_3$ and KNO_3 aqueous solutions. Although the replacement of $NH_2(CH_3)_2^+$ by other ions is unfeasible in the self-assembly process, it can be finished by the ion-exchange experiment conducted on the obtained compound. This research may exploit facile entry for an incorporation specified component into complex for the preconceived need in material design. Furthermore, magnetic property measurements on complexes **1**, **2**, and **5** indicate there exists weak antiferromagnetic interactions between magnetic centers in all three compounds.

ASSOCIATED CONTENT

Supporting Information. IR curves, magnetic data, powder diffraction patterns, TGA curves and table of selected bonds for complexes **1**−**7**. This material is available free of charge via the Internet at http://pubs.acs.org.

AUTHOR INFORMATION

Corresponding Author
*E-mail: rcao@fjirsm.ac.cn.

ACKNOWLEDGMENT

This work was financially supported by (2011CB932504, 2007CB815303), NSFC (20731005, 20821061, 91022007), NSF of Fujian Province (E0520003), and Key Projects from CAS.

REFERENCES

(1) (a) Zhang, W.; Ye, H.-Y.; Xiong, R.-G. *Coord. Chem. Rev.* **2009**, *253*, 2980. (b) Li, K.; Olson, D. H.; Seidel, J.; Emge, T. J.; Gong, H.; Zeng, H.; Li, J. *J. Am. Chem. Soc.* **2009**, *131*, 10368. (c) Liu, T.; Zhang, Y.-J.; Wang, Z.-M.; Gao, S. *J. Am. Chem. Soc.* **2008**, *130*, 10500. (d) Férey, G. *Chem. Soc. Rev.* **2008**, *37*, 191. (e) Kitagawa, S.; Kitaura, R.; Noro, S. *Angew. Chem., Int. Ed.* **2004**, *43*, 2334.

(2) (a) O'Keeffe, M.; Peskov, M. A.; Ramsden, S. J.; Yaghi, O. M. *Acc. Chem. Res.* **2008**, *41*, 1782. (b) Perry, J. J., IV; Perman, J. A.; Zaworotko, M. J. *Chem. Soc. Rev.* **2009**, *38*, 1400.

(3) (a) Kim, J.; Chen, B. L.; Reineke, T. M.; Li, H.; Eddaoudi, M.; Moler, D. B.; O'Keeffe, M.; Yaghi, O. M. *J. Am. Chem. Soc.* **2001**, *123*, 8239–8247. (b) Nouar, F.; Eubank, J. F.; Bousquet, T.; Wojtas, L.; Zaworotko, M. J.; Eddaoudi, M. *J. Am. Chem. Soc.* **2008**, *130*, 1833. (c) Yaghi, O. M.; O'Keeffe, M.; Ockwig, N. W.; Chae, H. K.; Eddaoudi, M.; Kim, J. *Nature* **2003**, *423*, 705.

(4) (a) Zhang, C. J.; Su., C. *Eur. J. Inorg. Chem.* **2007**, 2997. (b) Rabone, J.; Yue, Y.-F.; Chong, S. Y.; Stylianou, K. C.; Bacsa, J.; Bradshaw, D.; Darling, G. R.; Berry, N. G.; Khimyak, Y. Z.; Ganin, A. Y.; Wiper, P.; Claridge, J. B.; Rosseinsky, M. J. *Science* **2010**, *329*, 1053.

(5) (a) Sun, D.; Ma, S.; Ke, Y.; Petersen, T. M.; Zhou, H.-C. *Chem. Commun.* **2005**, 2663. (b) An, J.; Rosi, N. L. *J. Am. Chem. Soc.* **2010**, *132*, 5578. (c) Higuchi, M.; Tanaka, D.; Horike, S.; Sakamoto, H.; Nakamura, K.; Takashima, Y.; Hijikata, Yuh.; Yanai, N.; Kim, J.; Kato, K.; Kubota, Y.; Takata, M.; Kitagawa, S. *J. Am. Chem. Soc.* **2009**, *131*, 10336.

(6) Yang, S.; Lin, X.; Blake, A. J.; Thomas, K. M.; Hubberstey, P.; Champness, N. R.; Schröder, M. *Chem. Commun.* **2008**, 6108.

(7) (a) Plabst, M.; McCusker, L. B.; Bein, T. *J. Am. Chem. Soc.* **2009**, *131*, 18112. (b) Carlucci, L.; Ciani, G.; Maggini, S.; Proserpio, D. M.; Visconti, M. *Chem.—Eur. J.* **2010**, *16*, 12328.

(8) (a) Guo, Z.-G.; Cao, R.; Wang, X.; Li, H.; Yuan, W.; Wang, G.; Wu, H.; Li, J. *J. Am. Chem. Soc.* **2009**, *131*, 6894. (b) Liu, T.-F.; Lü, J.; Guo, Z.-G.; Proserpio, D. M.; Cao, R. *Cryst. Growth Des.* **2010**, *10*, 1489. (c) Liu, T.-F.; Lü, J.; Xi, L.and Cao, R. *Chem. Commun.* **2010**, *46*, 8439.

(9) (a) Kim, H.; Suh, M. P. *Inorg. Chem.* **2005**, *44*, 810. (b) Thallapally, P. K.; Tian, J.; Kishan, M. R.; Fernandez, C. A.; Dalgarno, S. J.; McGrail, P. B.; Warren, J. E.; Atwood, J. L. *J. Am. Chem. Soc.* **2008**, *130*, 16842. (c) Kishan, M. R.; Tian, J.; Thallapally, P. K.; Fernandez, C. A.; Dalgarno, S. J.; Warren, J. E.; McGrail, B. P.; Atwood, J. L. *Chem. Commun.* **2010**, *46*, 538. (d) Liang, L.-L.; Ren, S.-B.; Wang, J.; Zhang, J.; Li, Y.−Z.; Du, H.−B.; You X.−Z. *CrystEngComm* **2010**, *12*, 2669. (e) Tian, J.; Motkuri, R. K.; Thallapally, P. K. *Cryst. Growth Des.* **2010**, *10*, 3843.

(10) *CrystalClear*, version 1.36; Rigaku Corporation/MSC: The Woodlands, TX, 2000.

(11) Sheldrick, G. M. *SHELXS-97, Program for Crystal Structure Solution and Refinement*; University of Göttingen: Göttingen, Germany, 1997.

(12) Spek, A. L. *Appl. J. Crystallogr.* **2003**, *36*, 7.

(13) Burrows, A. D.; Cassar, K.; Düren, T.; Friend, R. M. W.; Mahon, M. F.; Rigby, S. P.; Savaresea, T. L. *Dalton Trans.* **2008**, 2465.

(14) Blatov, V. A. *IUCr CompComm. Newsletter* **2006**, *7*, 4; see also http://www.topos.ssu.samara.ru.

(15) Yang, J.; Li, G.-D.; Cao, J.-J.; Yue, Q.; Li, G.-H.; Chen, J.-S. *Chem.—Eur. J.* **2007**, *13*, 3248.

(16) (a) Kurmoo, M. *Chem. Soc. Rev.* **2009**, *38*, 1353. (b) Holman, K. T.; Hammud, H. H.; Isber, S.; Tabbal, M. *Polyhedron* **2005**, *24*, 221.

(17) (a) . Kahn, O. *Molecular Magnetism*; VCH: Weinheim, Germany, 1993. (b) Mondal, K. C.; Sengupta, O.; Nethaji, M.; Mukherjee, P. S. *Dalton Trans.* **2008**, 767. (c) Su, S.; Guo, Z.; Li, G.; Deng, R.; Song, S.; Qin, C.; Pan, C.; Guo, H.; Cao, F.; Wang, S.; Zhang, H. *Dalton Trans.* **2010**, *39*, 9123.

(18) (a) Menage, S.; Vitols, S. E.; Bergerat, P.; Codjovi, E.; Kahn, O.; Girerd, J. J.; Guillot, M.; Solans, X.; Calvet, T. *Inorg. Chem.* **1991**, *30*, 2666. (b) Adams, H.; Fenton, D. E.; Cummings, L. R.; McHugh, P. E.; Ohba, M.; Okawa, H.; Sakiyama, H.; Shiga, T. *Inorg. Chim. Acta* **2004**,

357, 3648. (c) Rardin, R. L.; Poganiuch, P.; Bino, A.; Goldberg, D. P.; Tolman, W. B.; Liu, S.; Lippard, S. J. *J. Am. Chem. Soc.* **1992**, *114*, 5240.

(19) Cui, H.; Otsuka, T.; Kobayashi, A.; Takeda, N.; Ishikawa, M.; Misaki, Y.; Kobayashi, H. *Inorg. Chem.* **2003**, *42*, 6114.